The influence of magnetic turbulence on Internal Transport Barriers of Reversed Field Pinch.

R. Lorenzini, F. Auriemma, A. Fassina, E. Martines, B. Momo, D. Terranova, Y. Zhang
Consorzio RFX – Associazione Euratom-ENEA – Padova, Italy

Introduction Quasi-Single Helicity (QSH) state, where a single mode dominates the secondary ones, has been widely observed in Reversed Field Pinch devices. In high current shots (I_p > 1.2 MA) of the RFX-mod experiment [1] QSH states routinely host thermal structures, enclosed by steep temperature gradients interpreted as electron Internal Transport Barriers (eITB). The spatial extent of thermal structures varies significantly; usually they are narrow and located off axis, while some of them are wide enough to enclose the geometrical axis. To date, such differences have been correlated to the topology of the magnetic field, determined by the combination of the axisymmetric equilibrium field with that due to the dominant mode. In earlier studies [2] a systematic presence/absence of a separatrix is found in narrow/wide thermal structures. Considering the theoretical result that the X-point favors the development of chaos generated by additional perturbations, the abrupt transition from narrow to wide thermal structures was ascribed to the separatrix disappearance. Recent results changed this vision, showing that the size W_{Te} of thermal structures features a regular increasing trend, shown in Fig 1, with the dominant mode amplitude even across the DAx-SHAx (Double Axis to Single Helical Axis) transition [3]. The difference between the past and the present results is due to the upgrade, accomplished just after the publication of [2], of the code that calculates the helical equilibrium. In [2] the parameters used in the computation of the main axisymmetric field were calculated in cylindrical approximation, while afterwards the calculation is in full toroidal geometry. This improvement allowed us to verify that the electron temperature, such as the density and the radiation, are flux functions [4]. The behavior of ITB gradients (Fig 2) tells us a symmetric story: as long as the dominant mode

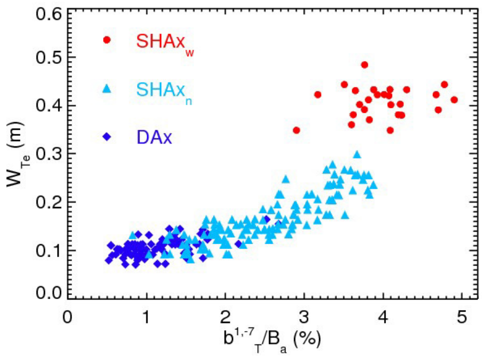

Figure 1. Thermal structure width W_{Te} vs the normalized amplitude of the dominant mode

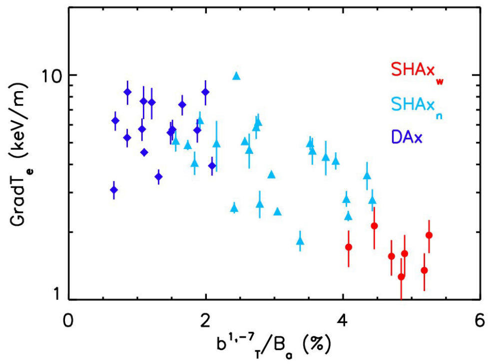

Figure 2. Minimum average gradient (between left and right average gradients) vs the dominant mode

increases the gradients become milder and show no discontinuity even across the DAx to SHAx transition [5].

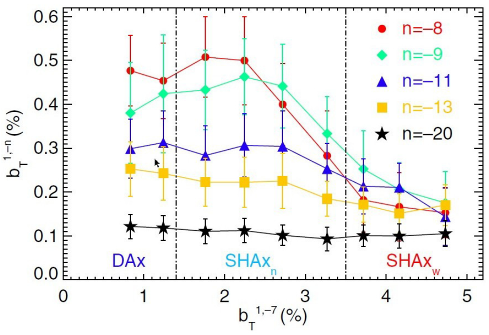

Figure 3 Ensamble-averaged spectrum of secondary modes vs the dominant one

How magnetic turbulence influences the extension W_{th} of thermal structures. The behaviour of secondary modes has been studied on a database of about 230 thermal structures measured with the TS diagnostics [6], whose line of sight is along the machine horizontal diameter. The ensamble-averaged spectrum of m=1 secondary modes (Fig.3) shows a decrease of their amplitudes, especially for the two innermost resonant, subdominant modes n=−8,−9, when $b^{1,-7}_T$ > 2.5% of B(a); in particular, the n=−8 mode, which usually is the largest one, becomes comparable to the other modes with a higher toroidal number in the SHAx$_w$ spectra. Since the island width is proportional to the mode amplitude, the SHAx$_w$ plasmas feature the smallest n=−8,−9 islands. This in turn suggests that SHAx$_w$ structures might occur when the reduced overlapping of n=−8,−9 mode islands mitigates the field stochasticity between the two resonance radii. This hypothesis is supported by the result that the positions ρ_8 and ρ_9 of the n=−8,−9 mode resonances on the helical q profile [7], are external to the ITB outermost points (ρ_{TH}) in DAx and SHAx$_n$ structures ($\rho_{8,9}$>ρ_{TH}). Conversely, SHAx$_w$ structures include ρ_8, so that the ITB gradients lie between the two resonances (ρ_8<ρ_{TH}<ρ_9). This implies that, in the latter case, the stochasticity is mitigated due to the smaller island size.

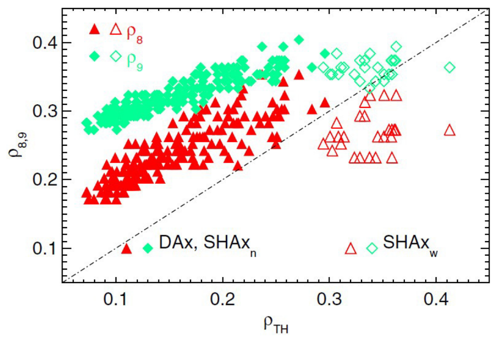

Figure 4 n=-8,-9 mode resonance position vs the position of most external points of ITB

How magnetic turbulence influences the gradients and the transport in ITBs. To analyse the thermal gradients we used a subset of profiles whose density varies between 2.5 and 3.5 10^{19}m^{-3}, and whose plasma current varies from 1.2 to 1.5 MA. The poloidal angle of the island O-point varies between -25 and 25 or 155 and 205 degrees. The additional requirement that the profiles have a very low scattering of data reduces significantly, to only 45, the number of ITB profiles in such database. The left/right average gradients of the ITB are calculated using

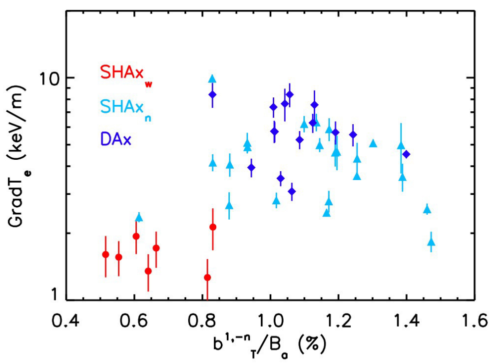

Figure 5 The minimum Te gradient is plotted versus the normalized secondary modes.

the simple linear combination of positions and T_e values of the ITB foot and top. Steepest gradients are found in the side where the O-point of the islands lies in the case of DAx, or where the helical axis lies in the case of $SHAx_{n,w}$. The plots in Fig. 2 and in Fig. 5 show the behaviour of the minimum (less steep) between the left and right gradient. The plots refer to the minimum gradient, since it is measured with more TS points than the maximum one, spanning a wider region. Despite the scattering of the data, Fig. 5 shows that the dependence of gradients from the secondary modes has two distinct regions. When $b^{1,-n}{}_{sec}>0.9\%$ the gradients become steeper as long as the energy of magnetic turbulence decreases, in agreement with the conjecture of stochastic transport. However when the magnetic turbulence becomes lower ($b^{1,-n}{}_{sec}<0.9\%$) the gradients become suddenly milder. The results shown in the previous paragraph allow interpreting also this result in the light of stochastic transport. In fact, the ITB gradients in $SHAx_w$ are located more externally than in DAx and $SHAx_n$ states, hence they are likely to be more sensitive to the stochasticity induced by the overlapping of packed and numerous, although small, magnetic islands of high n modes.

The Quasi Separatrix Layer concept: a way to quantitatively explain the W_{th} behavior. Fig. 1 shows that, contrary to what claimed in [2], the separatrix espulsion cannot be anymore considered as the sufficient condition to obtain the transition from a narrow to a wide thermal structure. This result motivated the idea of looking for a different interpretation of such process, based on an alternative theoretical interpretation. Such interpretation has been provided through the Quasi Separatrix Layer (QSL) model, widely used in the physics of solar flares to explain the occurrence of the magnetic reconnection without X-points [8]. The concept of separatrix has been generalized in 3D configurations to quasi-separatrix layers, defined as regions where there is a continuous, significant change of field line linkage [9]; if a separatrix exists it is part of the QSL as a particular case of discontinuous field line linkage. Considering the lines that connect photospheric areas of positive and negative magnetic polarities through a map, a QSL is found where such a mapping results in a squashing of the flux tube cross sections, for example, when a tiny circular region is mapped to a very elongated elliptical region. In analogy to solar physics, we assume that in our plasma quasi-separatrix layers behave physically like separatrices; the squashing of flux tubes becomes the global property that plays the role of seed for the chaos induced by magnetic perturbations. The flux tube squashing is defined through the dilatation that an infinitesimal area element dS, enclosed between two magnetic surfaces, undergoes when moving poloidally from a position where the surfaces are compressed to one where they are stretched. The surface dilatation is defined as the ratio between the "stretched" area $dS_s = dr_s \times dL$ and the "compressed" area $dS_c = dr_c \times dL$ (Fig. 6). The indicator D is the surface dilatation compensated by the flux tube expansion due to the toroidal magnetic field. The QSL is located where D assumes its highest values, indicating that the shape of surfaces is rapidly varying. The QSL extension is determined by a threshold value D_{th}, which should take into account the strength of magnetic perturbation. D_{th} has been taken as inversely proportional to the width $\Delta_{1,-8}$ of the n = −8 mode magnetic island, which is closest to the thermal gradients: D_{th}=A $(b_{r,res}{}^{1,-8})^{0.5} \propto \Delta_{1,-8}$, where $b_{r,res}{}^{1,-8}$ is n=-8 mode radial field at the resonance radius and A is a constant whose value is fixed, matching W_{Te} and W_{QSL} in a few reference $SHAx_n$ cases with $b_T{}^{1,-7}$~2%. The dependence of the threshold on $b_{r,res}{}^{1,-8}$ allows us to well reproduce the increasing trend of W_{Te} with its slope change observed at $b_T{}^{1,-7} \geq 2.\%$, as shown in Fig.7. Moreover, when the QSL model is applied to $SHAx_w$ cases, D_{th} is typically higher than the maximum value of D; hence, in $SHAX_w$, no stochastic QSL is found.

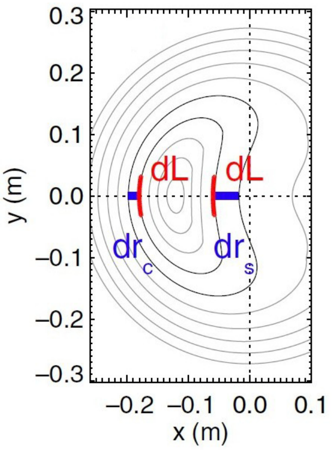

Figure 6 Depiction of variables used to define the indicator D

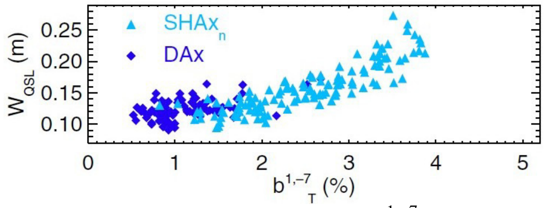

Figure 7 W_{QSL} plotted (a) versus $b_T{}^{1,-7}$

Conclusions. This paper aims at giving a detailed description of how the magnetic turbulence influences the characteristics of ITBs of RFX-mod, in particular the gradients of ITBs and the width of thermal structures enclosed by them. These results open promising scenarios for RFP machines where the magnetic turbulence could be more efficiently controlled, as in the forthcoming RFX-mod2 experiment that will be characterized by a lower shell proximity than RFX-mod. In such case we expect to observe routinely $SHAx_w$ structures, possibly with steeper ITBs than in RFX-mod. In still more promising scenario, provided that the n=-9,-10 are efficiently stabilized, we could obtain a further widening of $SHAx_w$ thermal structures.

Acknowledgment. *This work was supported by the European Communities under the contract of Association between EURATOM/ENEA. The views and the opinions expressed herein do not necessarily reflect those of the European Commission.*

References

[1] P. Sonato *et al.*, Fusion Engineering and Design 66,161 (2003)
[2] R. Lorenzini *et al.,* Phys. Rev. Lett. **101**, 025005 (2008)
[3] R. Lorenzini *et al.,* Phys. Rev. Lett. **116**, 185002 (2016)
[4] R. Lorenzini *et al.,* Nat. Phys. **5**, 570 (2009)
[5] Y. Zhang *et al.,* submitted to PPCF
[6] B. Momo *et al.,* Plasma Phys. Controlled Fusion **53**, 125004 (2011)
[7] A Alfier and R Pasqualotto, RSI 78(1),013505, (2007)
[8] P. Démoulin, *et al.,* Astron. Astrophys. **285**, 1023 (1994).
[9] P. Démoulin, *et al.,* J. Geophys. Res. 101, 7631 (1996).